Egyptian Knowledge Bank
https://ijmti.journals.ekb.eg/

International Journal of
Materials Technology and Innovation
Volume 2, Issue 2 (2022), pages 38-46

Online ISSN 2682-4299

Hybrid Composite Foams Based on Pb Alloys for Lightweight Batteries

A. Daoud [1,*], Atef Y. Shenoud [2], M.T. Abou El-Khair[1], F. Fairouz[1], E. Mohamed[1], M. E. Abdel Aziz[1]

[1] Composite Materials Dept., Central Metallurgical Research and Development Institute, P.O. Box 87, Helwan, Cairo, Egypt
[2] Chemical and Electrochemical Metallurgy Dept., Central Metallurgical Research and Development Institute, Helwan, Cairo, Egypt

*Corresponding author: E-mail: ADAOUD_eg@yahoo.com

Received 31 October 2022
Accepted 10 November 2022
Published 31 December 2022

Abstract

A low-cost direct melt foaming approach was used to develop a new Pb alloy-based composite foam comprising hybrid of gas pores and closed cell porosity in the form of hollow ceramic particles to be an alternative to the traditional Pb grids in Lead acid battery (LAB). The novel Pb alloy-based composite foams were used as plates to manufacture lightweight LAB. The LAB was evaluated regarding weight saved and electrochemical performance, including cyclic voltammetry, galvanostatic polarization, and specific discharge capacity. The cyclic voltammetry results of the composite foams revealed that the composite foam required a higher voltage for oxidation, indicating that Pb oxidation occurred slower in the composite foams. Galvanostatic measurements showed that the composite foam took a long time to oxidize Pb into $PbSO_4$, implying that the battery developed in the current work would have a longer lifespan than a conventional LAB. The LAB made of composite foams had a greater specific electrical discharge capability than a conventional LAB. The density of the composite foam was significantly smaller than the traditional lead alloy, showing that the weight of the composite foam plate was low. These findings suggested that the LAB with plates made of composite foams developed in the current study can be a feasible alternative to traditional Pb grids used in LAB.

Keywords: Pb grid, Pb alloys based composite foams, lead acid battery, curing, cyclic voltammetry, galvanostatic polarization.

1. Introduction

The attention to exploring lightweight and high-performance batteries has grown due to several reasons such as environmental problems, limited fuel resources, and irrefutable climate change [1, 2]. Due to the characteristics of deep-rooted technology, cut price, good safety, recyclability, accessible maintenance, and consistent behavior, lead-acid batteries (LABs) have been widely utilized in numerous applications, keeping the greatest market share in all types of batteries. Despite the above, LABs have a set of performance limitations, including heavyweights, inadequate specific capacities, short lifespan, and limited utilization efficiency. one alternative for reducing the weight and increasing the utilization efficiency of the presently used LABs is to replace heavy Pb grids with lower density and better properties materials. The primary functions of the grids are to support active chemicals and conduct current. Grid materials that function well must meet the following criteria: acceptable mechanical properties, high conductivity, raw material costs, and environmentally friendly nature [3, 4].

There have been several studies done to change out the high-density Pb grids with lower-density metals or alloys. Commercially pure nickel sheets were employed as substrates for the electrodeposition of PbO_2. The PbO_2 electrodeposition was conducted on the Ni-substrate by galvanostatic anodic deposition in acidic Pb $(NO_3)_2$ solution in the existence of additives to be used as a positive electrode in LAB [5]. Although the Ni substrate has good electrical conductivity, its density is too high to accomplish a considerable weight reduction in the electrode. To be employed as an electrode in LAB, a polyurethane foam substrate was plated with lead. The authors have reported that the polyurethane foam plated with lead can enhance the utilization of the active material and the specific energy as well as discharge performance and cycle life of LAB [6].

In other studies, Pb or Pb alloy was electrodeposited on copper or carbon foam substrates to fabricate electrodes [7-14]. Using copper foam as the substrate and adding cerium to the electrodepositing solution under ultrasonic treatment, Dai et al. [7] synthesized electrodes by electrodeposition. The electrode had a three-dimensional reticulate structure with a specific surface area of around 5700 m^2. m^{-3} and a porosity of about 88.1 %. The cyclic voltammetry results showed that when employed as the negative electrode material in a LAB, the electrode has good stability. In another research, Pb alloy was electrodeposited on a copper-foam substrate to develop positive electrodes for LABs. The positive electrodes considerably improved the charge/discharge performance of the batteries and exhibited a better utilization efficiency of the positive active materials (PAM) [8].

Gyenge et al. [9] studied open-cell structures as current collectors for LABs based on vitreous carbon substrates electroplated with a Pb-Sn (1 wt.%) alloy. The authors suggested that electroplated reticulated vitreous carbon collectors could be used in LABs because of their cycling behavior and the adaptability of electrodeposition.

Graphite foams with high electrical and thermal conductivities, superior mechanical strength, and low density were developed and explored as viable current collector materials to replace Pb alloys for developing lightweight LABs. The graphite foam is electrochemically stable in the operating voltage range of the negative electrode. However, due to sulfuric acid intercalation into graphite, the graphite foam is not electrochemically stable in the operating voltage range of the positive electrode [10].

To deposit Pb layers on reticulated vitreous carbon and porous conductive carbon, Wrobel et al. [3] used a galvanic method. Pb layers electrodeposited on porous conductive carbon have enhanced properties and a more uniform thickness. Porous conductive carbon has been demonstrated to be as effective as reticulated vitreous carbon, indicating that porous conductive carbon can be used as negative and positive plates in LABs.

Fabrication of Pb or Pb-alloy foams has been attempted on a few occasions. Pb or Pb-alloy foams can be used as plates for LABs, according to the authors [15, 16].

Generally, all the above-suggested electrode materials and their synthesis techniques are overwhelmed by several drawbacks such as inadequate properties, technical manufacturing complexities, and excessive pricing. In this study, a low-cost direct melt foaming approach was used to develop a new Pb alloy-based composite foam comprising a hybrid of gas pores and hollow ceramic particles to act as an alternative to the traditional Pb grids to address these drawbacks. The novel Pb alloy-based composite foams were used in the manufacturing of LAB. The LAB was evaluated regarding weight saving and electrochemical performance, including galvanostatic polarization, cyclic voltammetry, and specific discharge capacity.

2. Experimental work

2.1 Materials Preparation of the composites

The stirring route and direct melt foaming were used to manufacture the composite foams. Pb alloys were utilized as matrix materials, while Ni-coated fly ash microballoons were employed as reinforcements, pores, and thickening agents. Pb alloys with uniformly dispersed Ni-coated fly ash microballoons were synthesized using the following procedures. In a steel crucible heated to 350°C, the Pb alloy was melted. Ca, Sn, and Al were added when the melt temperature reached 400°C, and the melt temperature was raised to 450°C. A stirrer made of stainless steel coupled to a variable-speed motor was introduced into the melt. 5 vol % Ni-coated fly ash microballoons were preheated at 200ºC for 2 hours. They were then incorporated into the vortex generated by stirring. To guarantee microballoons incorporation in the melt, the melt mixture was stirred for 1 minute after the microballoons were fully incorporated. The temperature of the melt was then reduced to 400°C. The foaming agent (white lead carbonate) powder was stirred into the melt. The slurry was forcefully agitated to disseminate the foaming agent powder and microballoons evenly. To enable the foaming agent to release gas bubbles, the molten metal was maintained at the foaming temperature for 3 minutes. Subsequently, compressed air was used to chill the composite foam suddenly. Table 1 gives the codes, compositions, and density of the investigated materials.

Archimedes method was used to determine the densities of the composite foams. All measurements were conducted on a precision research balance (resolution 0.00001 g).

Table 1. Codes and compositions of the investigated alloys and foams

Code	Material	Composition
PGLA	Positive grid lead alloy	Pb0.08Ca1.6Sn0.008Al
NGLA	Negative grid lead alloy	Pb0.07Ca0.5Sn0.008Al
PCFSI	Positive composite foam	Pb0.08Ca1.6Sn0.008Al-5 vol.% of Ni-coated fly ash microballoons
NCFSI	Negative composite foam	Pb0.07Ca0.5Sn0.008Al-5 vol.% of Ni-coated fly ash microballoons

2.2 Preparation of the electrodes

Lead oxide powder with some additives was used to prepare the lead oxide paste used for plate preparation. The composition of lead oxide and additives is presented in Table 2.

For preparing the electrodes, plates were cut from the investigated materials. As shown in Table2, the paste was made by mixing PbO and Pb powders (50 g lead oxide powder and 15 g free lead) with 5 g distilled water and 10 g (1M) H_2SO_4, which were added gradually and thoroughly to make a homogeneous paste. The plates were weighed before pasting and then the paste was applied on the plates. The plates were set for 72 hours at 25°C for curing as shown in Fig.1 (a) & (b). The formation procedure was conducted with a 1 M H_2SO_4 electrolyte. The charging current was steadily raised over 12 hours, ranging from 20 to 300 $mAcm^{-2}$ until complete formation was achieved, forming PbO_2 on the positive electrode and spongy Pb on the negative electrode as shown in Fig. 2.

Table 2. Composition of leady oxide and additives for positive and negative electrodes preparation

Composition	Negative plate	Positive plate
PbO	68.5%	69.8%
Free Pb	30%	30%
Graphite	-----	0.2%
$BaSO_4$	0.8%	-----
Sodium Lignin Sulphonate (SLS)	0.3%	-----
Carbon black	0.2%	-----
Carboxy methyl cellulose (CMC)	0.2%	-----

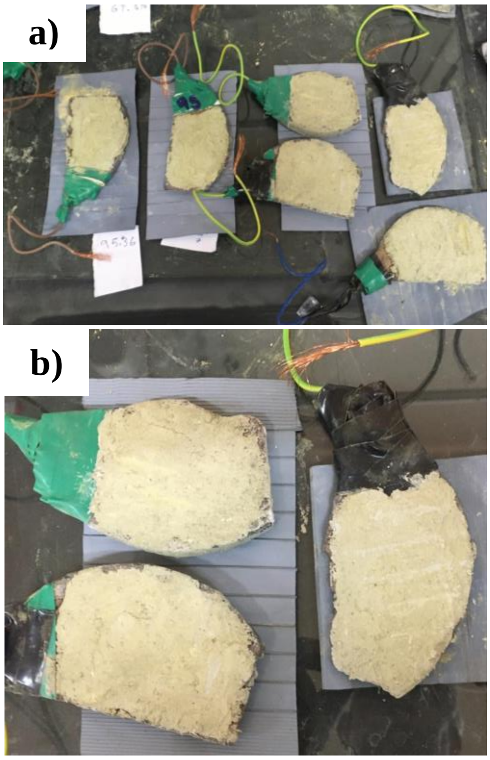

Fig. 1 Cured electrodes made of composite foams(a) and Higher magnification of cured plates made of composite foams (b)

Fig. 2 Formed positive (one lower) and negative (two upper) electrodes made of composite foams

2.3 Electrochemical measurements

Then, for cycle life measurements, the battery was charged at 20 $mAcm^{-2}$ for 3 h and discharged at 15 $mAcm^{-2}$ till the cut-off voltage of 1.75 V in 3M H_2SO_4, the specific discharge capacity was measured. DC Power Supply Topward (0-6A and 0-30V) was utilized to perform the specific discharge/charge galvanostatic measurement as shown in Figs. 3 and 4 (a &b).

Fig. 3 Battery with electrodes made of composite foams

For galvanostatic polarization and cyclic voltammetry measurements, the foam electrodes of 1 cm^2 cross-sectional area were reduced for about 3 minutes at the hydrogen evolution potential of -2V to remove any grease or oxidized residues. Then, at room temperature, cyclic voltammograms (CV) for composite foams were evaluated at a sweep rate of 1 mV/s in 3M H_2SO_4. The counter and reference electrodes were platinum wire and Hg/ Hg_2Cl_2/ KCl (SCE= 0.244 V vs. NHE), respectively. Galvanostatic polarization of the composite foams was studied at various current densities in 3M H_2SO_4. The steps of oxidation and reduction processes each took 60 and 45 minutes.

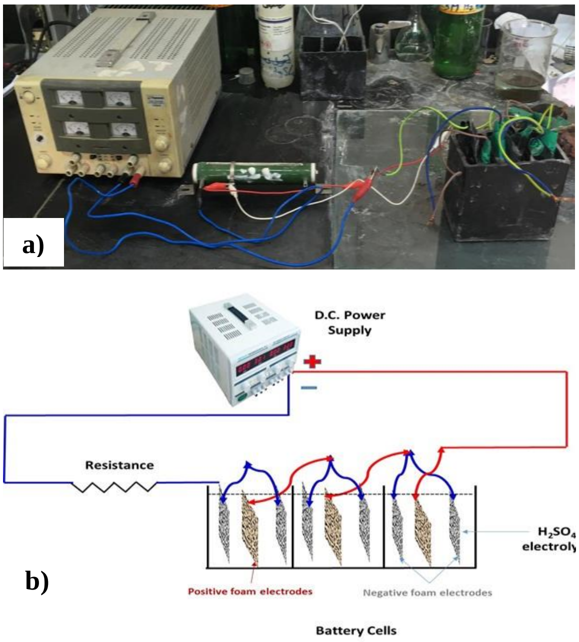

Fig. 4 Circuit including battery with electrodes made of composite foams (a) and schematic electrical circuit for the battery cells connection (b)

3. Results and Discussions

3.1 Density and porosity content

A representative macrostructure of the composite foam is shown in Fig. 5. The composite foam exhibits closed cells with uniform distribution and size of about 300 µm. Table 3 lists the densities, relative densities, and porosity percentage of the composite foams. The porosity percent (Pm) in the composite foam was determined using the measured density (ρ) of the composite foam as follows:

$$Pm=1-\rho/\rho s \times 100$$

where ρs is the density of dense Pb alloys and $\rho/\rho s$ is the relative density.

Table 3. Densities, relative densities, and porosity percentage of the composite foams

Material	Density (g/cm3)	Relative density (ρ/ρ_s)	Porosity percentage
PCFSI	2.35	0.21	79 %
NCFSI	2.65	0.23	77 %

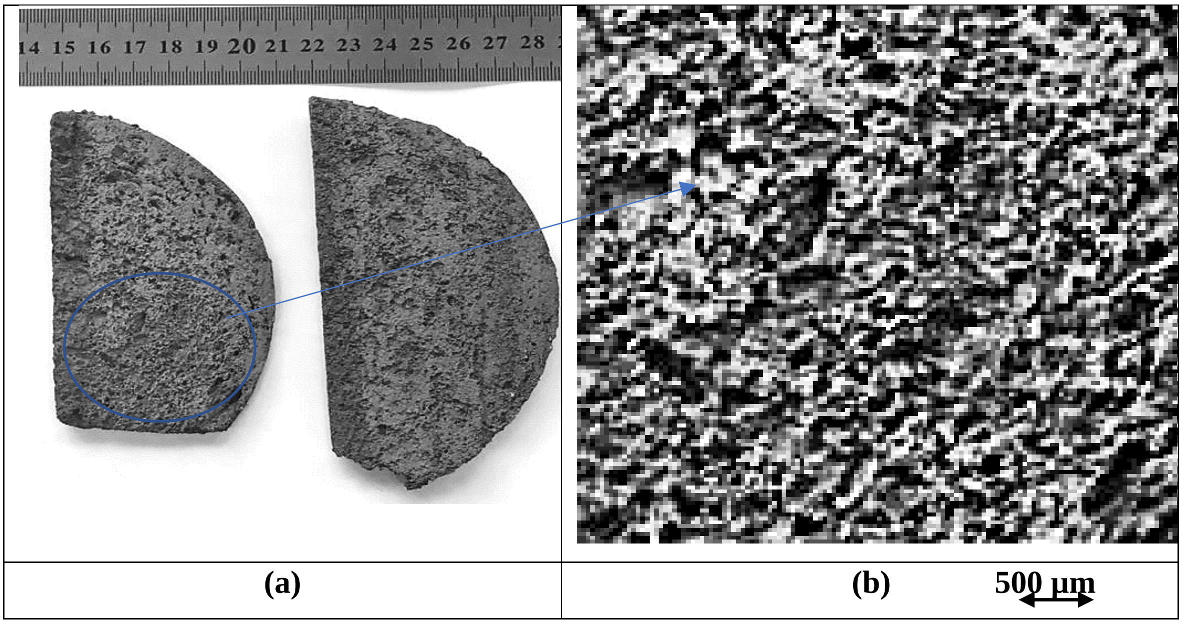

(a) **(b)**

Fig. 5 Plates cut from composite foams (a) and higher magnification view (b)

3.2 Cyclic voltammetric

The reversibility of the composite foams produced was studied using cyclic voltammetry (CV). Figs. 6 and 7 show the cyclic voltammogram for PCFSI and NCFSI electrodes at the potential range of -0.8 to +2 V vs. SCE in 3M H_2SO_4. CV of PCFSI has a strong anodic peak (A1) at -0.417 vs. SCE, corresponding to the mixed oxidation potentials (-0.172Vvs. NHE) of Pb to $PbSO_4$ and Pb to $PbO.PbSO_4$, respectively as explained by the following equations [17-19]:

$Pb + H_2SO_4 = PbSO_4 + 2H^+ + 2e^-$
$E_h = -0.356 - 0.029\ pH - 0.029$ (1)

$2Pb + H_2SO_4 + H_2O = PbO.PbSO_4 + 4H^+ + 4e^-$
$E_h = -0.115 - 0.029\ pH - 0.015\ \ln a_{[SO_4{}^{2-}]}$ (2)

Where pH is equal to $-\log_{10} c$, c is the hydrogen ion concentration in moles per liter, $a_{[SO_4{}^{2-}]}$ is the activity concentration of the sulphuric acid, E_h is the potential at the given pH of Pourbaix diagram, and ln is the natural logarithmic of the activity to the base of the mathematical constant e value (2.718).

Also, there is a second anodic peak (A2) at about 0.0V (0.247 V vs. NHE), corresponding to the oxidation potential of Pb to PbO as explained by the following equation:

$Pb + H_2O = PbO + 2H^+ + 2e^-$
$E_h = 0.248 - 0.059\ pH$ (3)

Finally, there is a third small anodic peak (A3) at 1.444 V (1.689 V vs. NHE), corresponding to the oxidation potential of $PbSO_4$ to PbO_2 as explained by the following equation:

$PbSO_4 + 2H_2O = PbO_2 + SO_4{}^{2-} + 4H^+ + 2e^-$
$E_h = 1.685 - 0.118\ pH + 0.029\ \lg a_{[SO_4{}^{2-}]}$ (4)

The cathodic reduction of the PCFSI shows three cathodic peaks (C1, C2, and C3) at -0.507, -0.321and 1.498V vs. SCE, respectively. The first cathodic peak (C1) occurs at 0.263 V vs. NHE according to the following reduction reactions:

$PbSO_4 + 2H^+ + 2e^- = Pb + H_2SO_4$
$E_h = -0.356 - 0.029\ pH - 0.029$ (5)

$PbO.PbSO_4 + 4H^+ + 4e^- = 2Pb + H_2SO_4 + H_2O$
$E_h = -0.115 - 0.029\ pH - 0.015\ \lg a_{[SO_4{}^{2-}]}$ (6)

This peak has mixed potentials for the reduction of $PbSO_4$and $PbO.PbSO_4$ into Pb.

The second cathodic peak (C2) at -77 mV vs. NHE is due to the reduction of $PbSO_4$and $PbO.PbSO_4$ into Pb according to following reactions:

$2PbO.PbSO_4 + 6H^+ + 6e^- = 3Pb + 2H_2SO_4 + H_2O$
$E_h = -0.075 - 0.029\ pH - 0.015\ \lg a_{[SO_4{}^{2-}]}$ (7)

The third cathodic peak (C3) at 1.75 vs. NHE is due to the reduction of PbO_2 into $PbSO_4$ as expressed by equation [18, 19]. On the other hand, the CV of NCFSI shows three anodic peaks (A1, A2 and A3) at -0.429, 0.003 and 1.404V for the oxidation of Pb to $PbSO_4$, Pb to $PbO.PbSO_4$, Pb to PbO, $PbSO_4$ to $2PbO.PbSO_4$, Pb and PbO_2 to $PbSO_4$. Also, similar behavior is obtained for the cathodic reduction of the NCFSI as observed in the PCFSI. There are three cathodic reduction peaks (C1, C2 and C3) at -0.507, -0.375 and 1.548V for the reduction of $PbSO_4$ & $PbO.PbSO_4$ to Pb, $2PbO.PbSO_4$ to Pb and PbO_2 to $PbSO_4$, respectively.

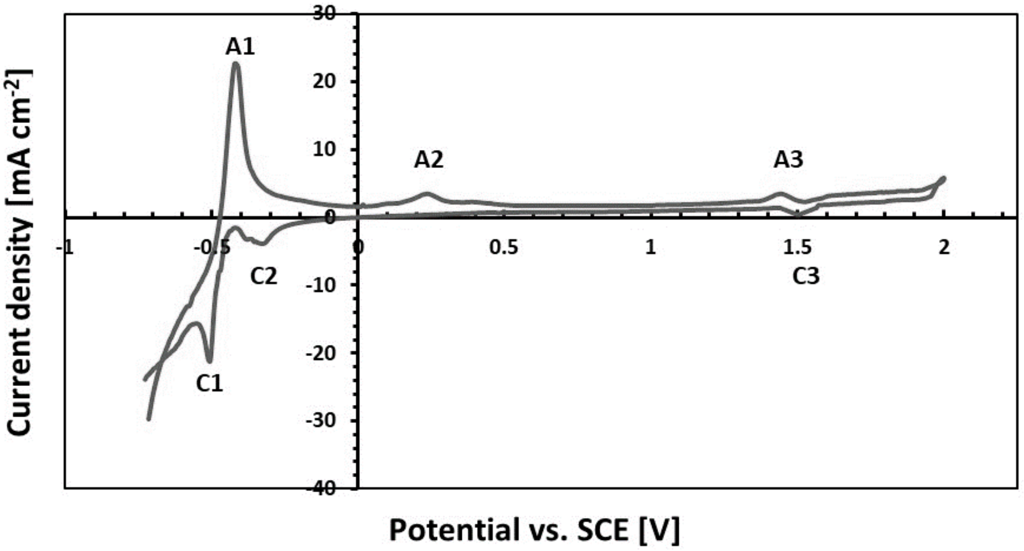

Fig. 6 CV of PCFSI in 3M H2SO4 at scan rate of 5 mVs-1

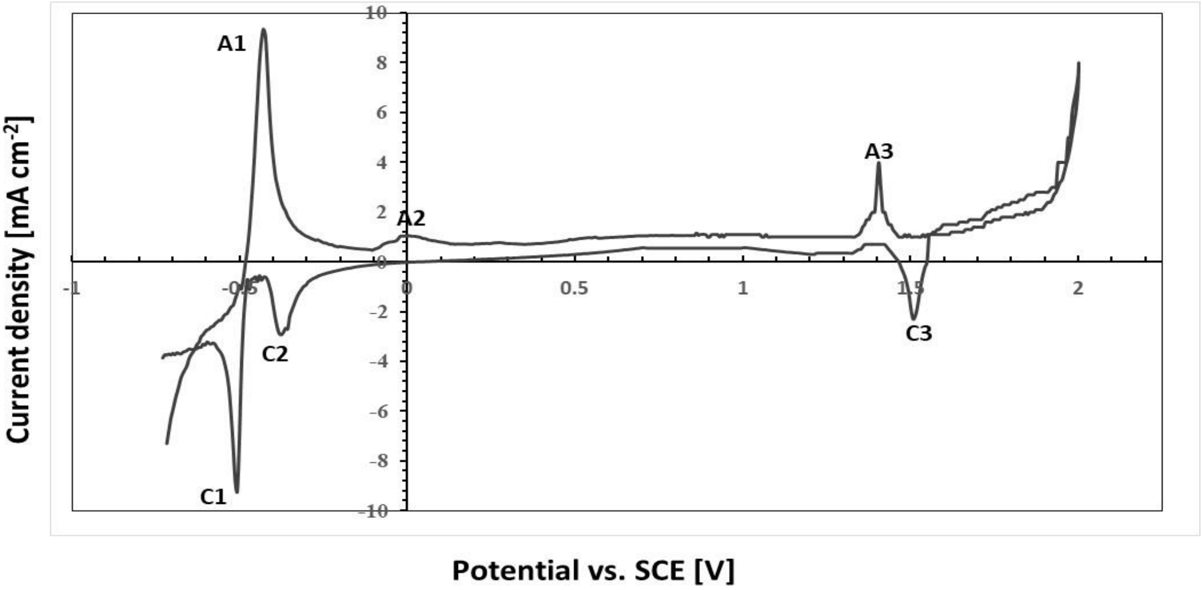

Fig. 7 CV of NCFSI in 3M H2SO4 at scan rate of 5 mVs-1

It's also worth noting that PCFSI's first anodic peak A1 has a higher current density (22 mAcm^{-2}) than NCFSI's (9 mAcm^{-2}). This confirms that the PCFSI has a higher reaction affinity for the H_2SO_4 electrolyte than the NCFSI, which has a lower affinity. This tendency can be explained by the fact that the PCFSI has a higher Sn percentage (1.6%) than the NCFSI (0.5%).

The cyclic voltammetry results for the composite foams reveal that the composite foam requires a higher voltage for oxidation. As a result, to match the high applied voltage for this oxidation, the oxidation of Pb into $PbSO_4$ will take a long time, i.e. Pb oxidation happens at a slower rate in composite foams than in Pb alloys [20]. As a result, it may be expected that the battery developed in the current study will last longer than a typical lead acid battery.

3.3 Galvanostatic polarization

The galvanostatic measurements were carried out to obtain E-t curves for the PCFSI and NCFSI polarization in 3 M H_2SO_4. Fig. 8 shows E-t relation for the PCFSI at numerous current densities (I_d) from 0.26 to 10 mA.cm^{-2}. At lower I_d, the first oxidation step of Pb to $PbSO_4$ takes place at -540 mV vs. SCE, but at higher I_d, this step occurs at ~ -500 mV. The second oxidation step of Pb into basic lead sulphates (BS) for lower I_d (0.26 mA.cm^{-2}) exists at -450 mV, while for I_d of 0.52 mA.cm^{-2} has ~ -300 mV. Furthermore, a high I_d of 2.6 mA.cm^{-2} has a higher potential between 20 and 50 mV for the second oxidation step. At this I_d, there is a third oxidation step that starts after 4000s and its potential varies between 50 and 110 mV for the oxidation of Pb to 3BS and 4BS, respectively. The galvanostatic polarization at higher I_d of 10 mA.cm^{-2} shows three oxidation steps from -500 to -200, 0 to 200 and 600 to 800 mV for Pb to $PbSO_4$, Pb to BSs & PbO and finally PbO to Pb_3O_4, respectively. The reduction steps for the different I_d have mainly reduction potential at -500 mV for lead basic sulphate and $PbSO_4$ to Pb. On the other hand, Fig. 9 shows E-t relation at the current density (I_d) of 20 mA.cm^{-2} for NCFSI. It can be noted that at higher I_d such as 20 mAcm^{-2}, the oxidation of lead has two steps, one at -540 mV for about 25 min due to oxidation of Pb to $PbSO_4$ and the other step is at -300 mV for the oxidation of Pb to 2 $PbO.PbSO_4$ with 65 min duration. The reduction behavior step takes place at about -540 mV but for higher I_d (20 mAcm^{-2}), it has a potential of -500 mV for the reduction of lead basic sulphates and $PbSO_4$ to Pb. The more reactive PCFSI rather than the NCFSI can explain the difference in galvanostatic polarization between the two foams, validating the findings obtained from the CV measurements of the two foams. Galvanostatic measurements show that the composite foam takes a longer time to complete the oxidation of Pb into $PbSO_4$ compared to the Pb alloys [20] because of the existence of fine cells (pores) in the structure of the foams as well as the existence of Ni- coated fly ash microballoons, which may impede the oxidation of the Pb element. Once more, this suggests that the battery produced in this work will last longer than a typical LAB.

3.4 Specific discharge galvanostatic

The cell made of composite foam electrodes has a specific electrical discharge capacity of approximately 113 mAh g^{-1}, which is greater than that of traditional Pb-grids, approximately 94 mAhg^{-1}. This is primarily due to the composite foam's large surface area, which is caused by the existence of fine cells (pores) in the structure of the composite foams. The connection between the composite foam electrode and the active material is increased due to the large surface area of the foam cells. This provides the active material more active reaction sites, which enhance the active material's conversion capability and electrochemical utilization efficiency [21].

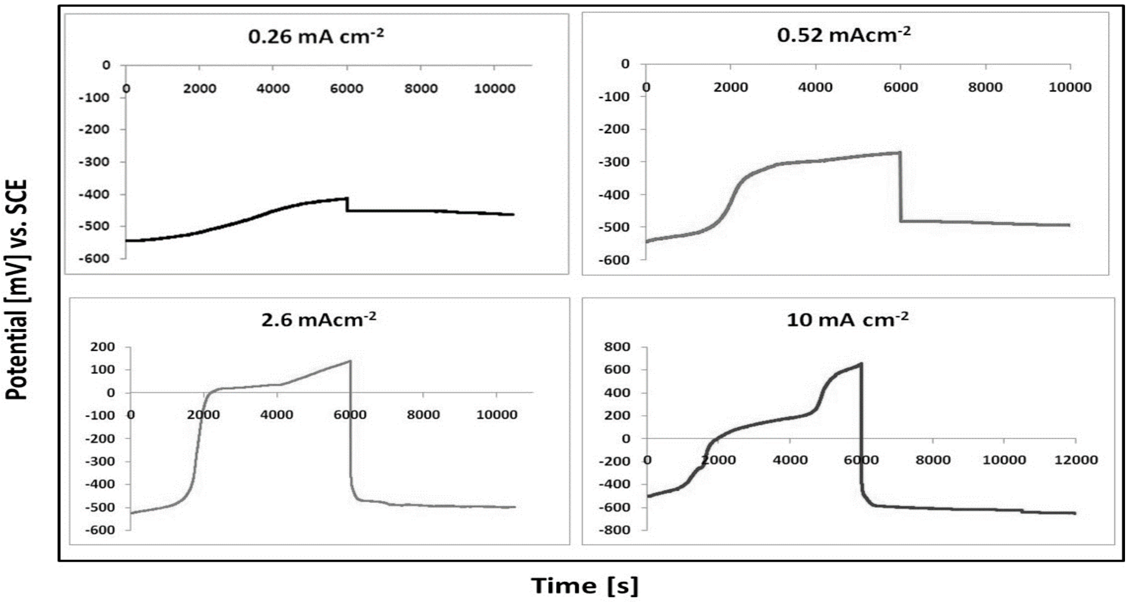

Fig. 8 E-t relation of galvanostatic polarization of PCFSI in 3 M H_2SO_4 at different current densities

Time [s]

Fig. 9 E-t relation of galvanostatic polarization of NCFSI in 3 M H_2SO_4 at current densities

3.5 Weight saving

The weights of electrodes made of the composite foam are less than the traditional lead alloys because the density of the foam is significantly lesser than that of the traditional Pb alloys. For instance, a traditional Pb grid with dimensions of 12 x 10 x 0.3 cm weighs 140 g, whereas a foam electrode with identical dimensions weighs 90 g. The weight savings would be roughly 35% if composite foam electrodes were used in place of the traditional Pb-grids.

4. Summary and conclusions

The cyclic voltammetry results for composite foams reveal that the composite foam requires a higher voltage for oxidation. As a result, to match the high applied voltage for this oxidation, the oxidation of Pb into $PbSO_4$ will take a long time, i.e. Pb oxidation happens at a slower rate in composite foams. This implies that the battery developed in the current work has a longer lifespan than a conventional LAB. Galvanostatic analysis reveals that the composite foam requires more time for Pb to oxidize into $PbSO_4$ than Pb alloys. This suggests once again that the battery developed in this work has a longer life expectancy than a regular lead acid battery.

The cells composed of composite foams have a larger specific electrical discharge capacity than conventional Pb grids. The composite foam electrodes developed in this work have improved galvanostatic polarization, cyclic voltammetry, specific discharge capacity as well as lower weight when compared to the Pb alloys used in conventional LAB. These characteristics are related to the composite foam's structure, which includes fine cells (pores) with a large surface area and Ni-coated fly ash microballoons. These findings suggest that the lead acid battery with electrodes made of composite foams developed in this work could be a feasible alternative to the traditional lead acid battery.

Acknowledgments

This paper is based upon work supported by Science, Technology & Innovation Funding Authority (STDF) under grant (EG-US: 42692). Also, this article is supported by USAID and NAS through Sub-award 2000010558.

References

[1] T. Yang, S. Qian, Y. Luo, X. Wang, Z. Wang, Direct Re-Usability of Lead-Plated Tin Bronze as Negative Plate for Lightweight Lead-Acid Battery, Journal of electrochemical Energy Conversion and Storage, 18 (2021) 030906. https://doi.org/10.1115/1.4050724
[2] A. Ilginis, N. Žmuidzinaviˇciene, E. Griškonis. Electrodeposition of Pb and PbO_2 on Graphite Felt in Membraneless Flow-Through Reactor: A Method to Prepare Lightweight Electrode Grids for Lead-Acid Batteries. Materials. 14 (2021) 6122. https://doi.org/10.3390/ma14206122
[3] K. Wrobel , J. Lach , J. Wrobel, P. Podsadni , A. Czerwinski. Journal of Power Sources Advances, 12 (2021) 00074. https://doi.org/10.1016/j.powera.2021.100074
[4] S. Jiang, Z. Song, A review on the state of health estimation methods of lead-acid batteries, Journal of Power Sources, 517 (2022) 230710.
[5] M.D. Hossain, M. M. Islam, M.J. Hossain, S. Yasmin, S. R. Shingho, N. A. Ananna, C. M. Mustafa, Effects of additives on the morphology and stability of PbO_2 films electrodeposited on nickel substrate for lightweight lead-acid battery application, Journal of Energy Storage, 27 (2020) 101108. https://doi.org/10.1016/j.est.2019.101108
[6] S.h. Chen li, W. bingbing, W. pengwei, Z. zhixue, Influence of specific surface area of foam lead grid on performance of lead acid batteries, Energy Storage Science and Technology, 9 (2020) 856-860.

[7] C.S. Dai, B. Zhang, D.L. Wang, T.F. Yi, X.G. Hu, Preparation and performance of Pb foam grid for negative electrode of VRLA battery, Materials Chemistry and Physics, 99 (2006) 431-436. https://doi.org/10.1016/j.matchemphys.2005.11.014

[8] K. Ji, C. Xu, H. Zhao, Z. Dai, Electrodeposited lead-foam grids on copper-foam substrates as positive current collectors for lead-acid batteries, Journal of Power Sources, 246 (2014) 307-316.

[9] E. Gyenge, J. Jung, B. Mahato, Electroplated reticulated vitreous carbon current collectors for Pb-acid batteries: opportunities and challenges, Journal of Power Sources. 113 (2003) 388-395, https://doi.org/10.1016/S0378-7753(02)00553-0

[10] Y.Il. Jang, N.J. Dudney, T.N. Tiegs, J.W. Klett, Evaluation of the electrochemical stability of graphite foams as current collectors for lead acid batteries, Journal of Power Sources, 161 (2006) 1392-1399.

[11] Y. Chen, B.Z. Chen, X.C. Shi, H. Xu, W. Shang ,Y. Yuan, L.P. Xiao. Preparation and electrochemical properties of pitch-based carbon foam as current collectors for lead acid batteries, Electrochimica Acta, 53 (2008) 2245-2249.

[12] Y. Chen, B.Z. Chen, L.W. Ma, Y. Yuan, Effect of carbon foams as negative current collectors on partial-state-of-charge performance of lead acid batteries, Electrochemistry Communications, 10 (2008) 1064-1066.

[13] L.W. Ma, B.Z. Chen , Y. Chen , Y. Yuan, Pitch-based carbon foam electrodeposited with lead as positive current collectors for lead acid batteries, Journal of Applied Electrochemistry, 39 (2009) 1609–1615. 10.1007/s10800-009-9852-z

[14] Y. Chen, B.Z. Chen, L.W. Ma, Y. Yuan, Influence of pitch-based carbon foam current collectors on the electrochemical properties of lead acid battery negative electrodes, Journal of Applied Electrochemistry, 38 (2008) 1409–1413. DOI: 10.1007/s10800-008-9580-9

[15] G. Costanza, M. Elisa Tata, Lead and lead alloys foams production, Acta Metallurgica Slovaca, 2 (2018) 347-352. DOI: https://doi.org/10.12776/ams.v24i4.1193.

[16] A. Irretier, J. Banhart, Lead and lead alloy foams, Acta Materialia, 53 (2005) 4903-4917. https://doi.org/10.1016/j.actamat.2005.07.007

[17] D. Pavlov, Lead-Acid Batteries: Science and Technology, Elsevier, First edition, (2011) 480.

[18] M. Dimitrov, D. Pavlov, Influence of grid alloy and fast charge on battery cycle life and structure of the positive active mass of lead-acid batteries, Journal of Power Sources, 93 (2001) 234- 257. https://doi.org/10.1016/S0378-7753(00)00598-X

[19] D. Pavlov, in: B.D. McNicol, D.A.J. Rand (Eds.), Power Sources for Electric Vehicles,Elsevier, (1984) 116–117.

[20] A. Daoud, M.T. Abou El-Khair; A.Y Shenouda, F. Fairouz, E. Mohamed, M.E. Abdel Aziz,; K. Yanamandra,; N. Gupta, Novel Pb alloys based composite foams containing hybrid pores produced by liquid metallurgy for lightweight batteries. Int. J. Lightweight Materials and Manufacturing, 5 (2022) 44–57.